Applied Catalysis B: Environmental 129 (2013) 325–332

Contents lists available at SciVerse ScienceDirect

Applied Catalysis B: Environmental

journal homepage: www.elsevier.com/locate/apcatb

Superoxide radical driving the activation of persulfate by magnetite nanoparticles: Implications for the degradation of PCBs

Guo-Dong Fang[a,d], Dionysios D. Dionysiou[b], Souhail R. Al-Abed[c], Dong-Mei Zhou[a,*]

[a] Key Laboratory of Soil Environment and Pollution Remediation, Institute of Soil Science, Chinese Academy of Sciences, Nanjing 210008, PR China
[b] Environmental Engineering and Science Program, University of Cincinnati, Cincinnati, OH 45221-0071, USA
[c] National Risk Management Research Laboratory, U.S. Environmental Protection Agency, 26 West Martin Luther King Drive, Cincinnati, OH 45268, USA
[d] Graduate School of the Chinese Academy of Sciences, Beijing 100049, PR China

ARTICLE INFO

Article history:
Received 16 July 2012
Received in revised form 28 August 2012
Accepted 24 September 2012
Available online 2 October 2012

Keywords:
MNPs
Superoxide radical
Activation
PS
Sulfate radical
PCB28

ABSTRACT

Magnetite nanoparticles (MNPs) are ubiquitous components of the subsurface environment, and increasing attention has been paid to MNPs due to their highly reductive and heterogeneous catalysis reactivity for the degradation of organic contaminants. However, most previous research studies neglected the generation of reactive oxygen species (ROS) by MNPs, which plays an important role in the transformation of contaminants. In this paper, we investigated the activation of persulfate (PS) by MNPs for the degradation of 2,4,4′-CB (PCB28), a selected model compound, and the underlying mechanism was elucidated. The results indicated that the PS can be activated by MNPs efficiently for the degradation of PCB28 at neutral pH. Electron paramagnetic resonance (EPR) technique was used to detect and identify the radical species in these processes. The mechanism of the activation of PS by MNPs was that superoxide radical anion ($O_2^{\bullet-}$) generated by MNPs could activate the PS to produce more sulfate radicals ($SO_4^{\bullet-}$), which favored the degradation of PCB28. The conclusion was further confirmed by quenching studies with the addition of superoxide dismutase (SOD). The effects of Fe(II) and pH on the degradation of PCB28 by PS/MNPs as well as the generation of ROS by MNPs were also studied. Both sorbed Fe(II) on MNPs surface and increased pH led to production of more $O_2^{\bullet-}$, which activated the PS to give more $SO_4^{\bullet-}$ to degrade PCB28. In addition, increasing the oxygen concentration in the reaction solution favored the generation of $O_2^{\bullet-}$ as well as the degradation of PCB28. The findings of this study provide new insights into the mechanism of heterogeneous catalysis based on MNPs and the reactivity of MNPs toward environmental contaminants.

1. Introduction

Increasing attention has been paid to sulfate radical due to its high efficiency for mineralization of organic pollutants [1–3]. It has been demonstrated that the persulfate (PS) can be activated by UV, heat, base, or transition metals to generate $SO_4^{\bullet-}$ [4]. However, only few studies have investigated the heterogeneous activation of PS by metal oxides, and the underlying mechanism was poorly understood [5,6]. Sulfate radical-based oxidation technologies have been applied to degrade various organic pollutants, but the degradation of PCBs by $SO_4^{\bullet-}$ has not been extensively studied [7,8,4,9]. Our recent study reported the transformation products of PCB28 as well as the proposed transformation pathways by $SO_4^{\bullet-}$ [10,11], thus, PCB28 was used as a model compound in this study.

The heterogeneous reduction of pollutants by ferrous iron (Fe(II)) is believed to be a key process influencing the fate and transformation of contaminants in the environment [12,13]. In recent years, studies have shown that a wide range of environmental contaminants can be reduced by Fe(II) absorbed to or within iron oxides, including goethite, magnetite, green rust, macjinawite, aluminum oxide, hematite and ferrrihydrite [14,15]. Especially, the reactivity of both absorbed and structural Fe(II) of magnetite has been extensively studied because of their ubiquitous presence in the subsurface environment [16,17]. Magnetite is an inverse spinel crystal structure with a unit cell composed of 32 O^{2-} anions, 16 Fe^{3+} cations, and 8 Fe^{2+} cations [18]. It is highly reactive with several contaminants including hexahydro-1,3,5-trinitro-1,3,5-triazine [14], carbon tetrachloride [16,17], nitrobenzene [15], hexavalent chromium and uranium [19,20]. Studies of the interaction between Fe(II) and mineral surfaces often focus on the catalytic effects for reductive transformation of organic and inorganic compounds. However, little attention has been paid to the role of oxygen (O_2) in these processes. O_2 can readily accept electron from Fe(II)

* Corresponding author. Tel.: +86 25 86881180; fax: +86 25 86881180.
E-mail address: dmzhou@issas.ac.cn (D.-M. Zhou).

0926-3373/$ – see front matter © 2012 Elsevier B.V. All rights reserved.
http://dx.doi.org/10.1016/j.apcatb.2012.09.042

to produce ROS, including $O_2^{\bullet-}$, hydrogen peroxide (H_2O_2) and $^{\bullet}OH$, which have important implications for the transformation of pollutants [21,22]. Recently, $O_2^{\bullet-}$ is of interest in environmental chemistry because of its potential to destroy highly toxic organic chemicals such as chlorinated solvents, pesticides, dioxins and other chemicals that are carcinogenic in majority of the cases [23]. $O_2^{\bullet-}$ can behave as a nucleophile toward alkyl halides, and displaces the halide from the carbon center via an S_N2 mechanism. $O_2^{\bullet-}$ reactivity toward $RCCl_3$ compounds is consistent with the single-electron-transfer mechanism [24].

In recent years, the use of zero-valent iron (ZVI) or Fe(II) to generate reactive oxidants such as $^{\bullet}OH$, Fe(IV) and $O_2^{\bullet-}$, by oxygen reduction has been proposed as a means of contaminant oxidation [25–29]. The generation of ROS can be described in the following reactions [30].

$$Fe^{2+} + O_2 \rightarrow O_2^{\bullet-} + Fe^{3+} \quad (1)$$

$$Fe^{2+} + O_2^{\bullet-} + 2H^+ \rightarrow Fe^{3+} + H_2O_2 \quad (2)$$

$$O_2^{\bullet-} + H^+ \leftrightarrow HO_2^{\bullet} \quad (3)$$

$$2O_2^{\bullet-} + 2H^+ \rightarrow H_2O_2 + O_2 \quad (4)$$

$$Fe^{2+} + H_2O_2 \rightarrow Fe^{3+} + {}^{\bullet}OH + {}^{-}OH \quad (5)$$

For example, the addition of Fe(II) to solutions containing As(III) resulted in oxidation of much of the As(III) to As(V) at pH 6.5–8.0 [31]. Surface-catalyzed Fe(II) oxidation by oxygen also has been proposed as means of oxidizing carbon tetrachloride and polyhalogenated methanes [32,33]. However, most of these studies did not provide direct evidence for the formation of the ROS in these processes, and the determination of the types and concentrations of ROS generated in these processes was not fully conducted. Furthermore, until now, it appears that no studies have been reported on the generation of ROS by magnetite, and little information is available in the literature.

More recently, MNPs have been widely reported as a suitable heterogeneous catalyst because of its magnetic and redox properties [34]. For instance, heterogeneous Fenton-like system, consisting of MNPs and H_2O_2, are effective for the degradation of organic compounds [34,35]. However, only few studies have dealt with the activation of persulfate by MNPs for the degradation of pollutants [6]. Therefore, the main objective of this study was to investigate the activation of PS by MNPs for the degradation of PCB28, and to elucidate the role of superoxide radical in this process. EPR technique was employed to identify the ROS generated in this processes. In addition, the effects of Fe(II), pH and O_2 on the degradation of PCB28 as well as the generation of ROS were also investigated.

2. Materials and methods

2.1. Chemicals

2,4,4′-Trichlorobiphenyl (2,4,4′-CB) was obtained from AccuStandard (New Haven, CT, UAS). 5,5-Dimethyl-1-pyrrolidine N-oxide (DMPO, 97%) was purchased from Sigma–Aldrich, Inc. Hexane (Chromatography grade) was obtained by CNW technologies GmbH, Germany. The rest of the chemicals, such as sodium persulfate (99%), sulfuric acid, sodium hydroxide, ferrous sulfate ($FeSO_4{\cdot}7H_2O$) and ferric chloride ($FeCl_3{\cdot}6H_2O$) were purchased from China National Medicines Corporation Ltd. (Beijing, China), and all of these chemicals were of analytical grade. 3-N-morpholino propanesulfonic acid (MOPS, 99.9%) and 2,2′-bipyridine (BPY, 99.9%) were purchased from J&K Scientific Ltd., China. Superoxide dismutase (SOD, 6.5×10^4 U/mg, 97%) was provided by Beyotime Institute of Biotechnology, China. Commercial magnetite nanoparticles (CMNPs) with average sizes of 20 nm, and Brunauer–Emmett–Teller (BET) surface area of 62 m^2/g were obtained from Nanjing Emperor Nano Material Co. Ltd., China, and were stored in an anaerobic glovebox (nitrogen protect system, YQX-II, Shanghai CIMO Medical Instrument Manufacturing Co. Ltd., China). Deionized water (DIW) with resistivity of 18 MΩ cm^{-1} was used as required in the experiments. The deoxygenated water was obtained from boiling DIW for 1 h at 100 °C, then sparging with nitrogen gas for an additional 1 h.

2.2. MNPs synthesis and characterization

MNPs were prepared by chemical coprecipitation method [36], as detailed in Supporting information (Text S1, Fig. S1). Fig. S1 shows the TEM image and size distribution of the MNPs, indicating that the MNPs are spherical with diameter ranging from 5 to 10 nm (average diameter: about 8 nm). XRD results showed diffraction peaks appeared at 2θ of 30.1°, 35.3°, 43.1°, 57.1°, and 62.8°, which are indicative of crystalline Fe_3O_4 (magnetite, JCPDS-19-0629). The specific surface area was measured as 83.5 ± 0.5 m^2/g by BET analysis with N_2 adsorption. Raman spectrum revealed a peak at 662 cm^{-1}, which is typical characteristic of magnetite (Fe_3O_4), not γ-Fe_2O_3.

2.3. Experimental procedures

Batch experiments were conducted in the 40 mL brown serum bottles capped with a Teflon Mininert containing 15 mL of reaction solution. Firstly, 1.0 mL MNPs stock solution (15 g/L, sonicated for 5 min to obtain well suspended particles) was dispersed into 13.9 mL aqueous solution of PCB28 (2.5 μM) at pH 7.0 (5.0 mM phosphate buffer, PBS) at 25 °C. Previous studies usually used the Good's buffers, such as MOPS and 4-(2-hydroxyethyl)-1-piperazine-ethanesulfonic (HEPES), for controlling pH due to the weak complexes of these buffers to Fe(II) [37]. But these Good's buffers could scavenge the ROS such as $^{\bullet}OH$ and $O_2^{\bullet-}$, thus PBS was used in this experiment. Then, the serum bottles were placed on a reciprocating shaker, to completely mix and achieve adsorption–desorption equilibrium for 1 h (the equilibrium time was obtained from the adsorption experiments). The degradation experiments were subsequently initiated by adding 0.1 mL persulfate solution (0.3 M) to the above reaction solution, and the serum bottles were placed on a reciprocating shaker (speed 150 rpm) at 25 °C. Compare experiments without PS or MNPs were also performed under identical reaction conditions. At each sampling event, the MNPs were separated from the sample with a magnet. Two milliliters of supernatant solution were sampled in 8 mL-serum bottles, and immediately 1.0 mL ethanol was added to quench the reaction, followed by addition of 2.0 mL hexane to extract PCB28. The extracted samples were analyzed by gas chromatography.

Experiments performed to investigate the effect of pH were conducted under identical conditions at different pH values adjusted using 1.0 M sodium hydroxide (NaOH) and hydrochloric acid (HCl). Fig. S2 shows that the MNPs have the maximum adsorption capacity of Fe(II) as its concentration was 2.0 mM in 2 h, thus, the concentration of Fe(II) used in adsorption experiment was 2.0 mM. Suspensions of MNPs with sorbed Fe(II) were prepared by adding $FeSO_4$ stock solution to anoxic suspensions of MNPs (1.0 g/L) in 10 mM MOPS (pH 7.0) and stirring the mixture for 8 h in an anaerobic glovebox under N_2 atmosphere (the final Fe(II) concentration was 2 mM). Then, MNPs were separated from the solution using a magnet and then rinsed with deoxygenated water to remove the remaining MOPS and $FeSO_4$. All these procedures were conducted in glovebox. After that, the experiments using MNPs-Fe(II) were performed under identical conditions to compare with the results obtained using MNPs. The effects of dissolved oxygen concentration

in reaction solution were investigated in experiments in which the water was sparged with air or N_2 for 1 h prior to the initiation of the reactions. All the experiments were carried out in triplicate, and the average values and the standard deviations are presented. EPR experiments were performed on a Bruker EMX 10/12 spectrometer (Germany) with DMPO as a spin-trapping agent. Detailed experiments and parameters can be seen in Text S2.

2.4. Analytic methods

The concentrations of PCB28 were determined by gas chromatography (GC/μECD, Aglient7890, USA) equipped with ^{63}Ni electron capture detection (ECD) and auto-sampler (Text S3). The EPR spectra were obtained using a Bruker EMX 10/12 spectrometer (Germany), and analyzed by WINEPR SimFonia software (Bruker, Germany). The degradation efficiency of PCB28 was calculated by the pseudo first-order kinetics equation (Text S3). The degradation efficiency of PCB28 was based on the concentration at the first sampling time after adsorption equilibrium was reached. Data from the recovery rate of PCB28 were analyzed by calculation of the means and standard deviations. All experimental data were processed with statistical software SPSS 11.5. Statistical significance is accepted when the probability of the result assuming the null hypothesis (p) is less than 0.05.

3. Results and discussion

3.1. The activation of PS by MNPs for the degradation of PCB28

Fig. 1(a) shows the degradation of PCB28 by PS with and without MNPs at pH 7.0 at 25 °C. Approximately 90% of PCB28 was degraded by PS/MNPs, whereas approximately 10% of PCB-28 was degraded by PS or MNPs alone. The dissolved Fe(II) from MNPs was also measured, which was below the detection limit, indicating that it was not the Fe(II) activating the PS for the degradation of PCB28.

It has been reported that the degradation of PCB28 was mainly ascribed to $SO_4^{\bullet-}$ in the PS/MNPs system [6], therefore, EPR technique was utilized to identify the ROS generated in these processes. As shown in Fig. 1(b), the hyperfine splitting constants of DMPO radical adducts in PS (obtained by simulation, a_N = 13.2 G, a_H = 9.6 G, a_H = 1.48 G and a_H = 0.78 G) were in agreement with literature data [38]. These are representative of $SO_4^{\bullet-}$ radicals added to DMPO (DMPO-SO_4), indicating that the $SO_4^{\bullet-}$ was predominant in the PS system. Meanwhile, the hyperfine splitting constant of DMPO radical adducts was a_N = 14.3 G, a_H = 11.2 G, and a_H = 1.3 G in the MNPs suspension. These are representative of $O_2^{\bullet-}$ radicals added to DMPO (DMPO-O_2), suggesting that the $O_2^{\bullet-}$ was predominant radical species in the MNPs suspension [39]. Additionally, the results revealed the formation of DMPO-SO_4 and DMPO-O_2 signals in the PS/MNPs system, indicating that the $SO_4^{\bullet-}$ and $O_2^{\bullet-}$ coexisted. Furthermore, the formation of DMPO-SO_4 signal in PS/MNPs was higher than that in PS, indicating that the concentration of $SO_4^{\bullet-}$ in PS/MNPs was higher than that in PS. On the other hand, the formation of DMPO-O_2 signal in PS/MNPs was lower than that in PS, suggesting that the concentration of $O_2^{\bullet-}$ in PS/MNPs was lower than that in MNPs. The results suggest that $O_2^{\bullet-}$ would participate in the reaction that generate $SO_4^{\bullet-}$. Previous studies have been reported that the reaction of $O_2^{\bullet-}$ with persulfate anion to generate $SO_4^{\bullet-}$ proceeds according to Eq. (6) [23].

$$S_2O_8^{2-} + O_2^{\bullet-} \rightarrow SO_4^{2-} + SO_4^{\bullet-} + O_2 \quad (6)$$

Therefore, it was hypothesized that the $O_2^{\bullet-}$ was a critical factor in controlling the generation of $SO_4^{\bullet-}$ by PS/MNPs. To further prove this hypothesis, experiments were conducted to observe the evolution of $SO_4^{\bullet-}$ and $O_2^{\bullet-}$ as function of time by EPR. Figs. 1(c) and S3 presents the details of the dynamics of the formation of

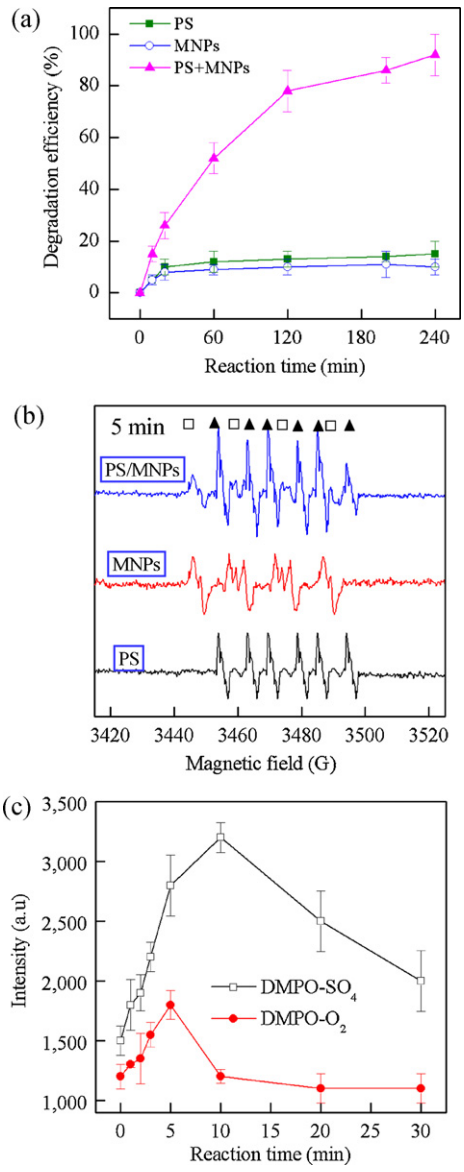

Fig. 1. The activation of PS by MNPs for the degradation of PCB28 (a). EPR spectrum of PS, MNPs, and PS/MNPs in the presence of 0.1 M DMPO after reaction for 5.0 min (b). Changes of the intensity of the formation of DMPO adducts as a function of time (c). Reaction conditions: [PS] = 2.0 mM, [PCB28] = 2.5 μM, [MNPs] = 1.0 g/L, 25 °C, pH 7.0 and reaction for 4 h; [DMPO] = 0.1 M.

DMPO-SO_4 and DMPO-O_2. The results showed that the formation of DMPO-O_2 increased rapidly from 0 to 5 min, and then decreased from 5 to 10 min, finally, slightly changed from 10 to 30 min. In contrast, the formation of DMPO-SO_4 increased rapidly from 0 to 10 min, and then decreased with increasing reaction time up to 30 min.

Two possible explanations would account for the above results. First, the oxidation of the surface or lattice Fe(II) was fast at the beginning of the reaction after adding PS, therefore, the formation of $O_2^{\bullet-}$ increased progressively. Although the reaction of $O_2^{\bullet-}$ and PS consumed the $O_2^{\bullet-}$, its consumption rate was lower than its formation rate. Thus, it was observed that the formation of DMPO-O_2 increased from 0 to 5 min. Meanwhile, the formation of DMPO-SO_4 increased rapidly from 0 to 5 min due to the high concentration of $O_2^{\bullet-}$, which reacts with PS to produce $SO_4^{\bullet-}$ radical. MNPs oxidation to γ-Fe_2O_3 results in coating the surface of MNPs, thus hindering the structural Fe(II) diffusion to the particle surface for further oxidation. Therefore, with reaction time from 5 to 10 min,

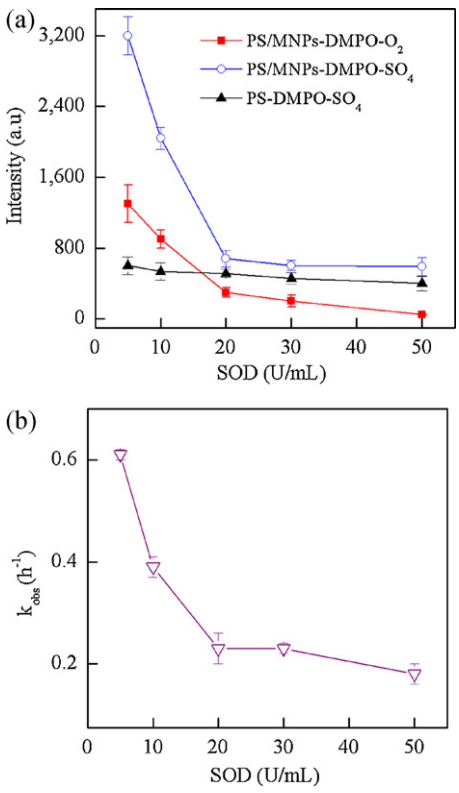

Fig. 2. Effects of the SOD concentrations on the intensity of the formation of DMPO adducts in PS, MNPs, and PS/MNPs at 10 min (a), and on the k_{obs} of PCB28 (b). Reaction conditions: [PS] = 2.0 mM, [PCB28] = 2.5 μM, [MNPs] = 1.0 g/L, 25 °C, pH 7.0 and reaction for 4 h; [DMPO] = 0.1 M, [SOD] = 5–50 U/mL.

the formation of DMPO-O_2 decreased. Second, the reaction of $O_2^{\bullet-}$ with PS resulted in the rapid formation of DMPO-SO_4 within 10 min. After that, the decrease of $O_2^{\bullet-}$ concentration and self-scavenging of $SO_4^{\bullet-}$ resulted in the reduction of $SO_4^{\bullet-}$ concentration as reaction time proceeded from 10 to 30 min.

In order to further scrutinize whether the generation of $SO_4^{\bullet-}$ by PS was drove by $O_2^{\bullet-}$, we investigated the effect of SOD, an enzyme which catalyzes the decomposition of $O_2^{\bullet-}$ to form H_2O_2 and O_2, on types of radical species generated by PS/MNPs. Figs. 2(a) and S4 present the effect of SOD on the formation of radical species in the PS and PS/MNPs systems. Both the formation of DMPO-O_2 and DMPO-SO_4 decreased rapidly as SOD concentration increased up to 20 U/mL, indicating that the presence of SOD markedly inhibited the generation of $SO_4^{\bullet-}$ and $O_2^{\bullet-}$ in the PS/MNPs system. However, the formation of DMPO-SO_4 slightly changed in PS in the presence of SOD, indicating that the SOD could hardly react with $SO_4^{\bullet-}$. Therefore, the inhibition of formation of $SO_4^{\bullet-}$ in the PS/MNPs was mostly attributed to the scavenging of $O_2^{\bullet-}$ by SOD, which resulted in the reduction of the generation of $SO_4^{\bullet-}$ through the reaction of $O_2^{\bullet-}$ and PS. These results further support the hypothesis that $O_2^{\bullet-}$ drives the generation of $SO_4^{\bullet-}$ in the PS/MNPs system. In addition, the effects of SOD on the degradation of PCB28 by PS/MNPs were also studied. As shown in Fig. 2(b), the k_{obs} decreased from 0.61 to 0.18 h^{-1} with an increase in SOD concentration up to 50 U/mL, indicating that the SOD greatly inhibited the degradation of PCB28. This is due to the scavenging of $O_2^{\bullet-}$ by SOD, which resulted in the reduction of the formation of $SO_4^{\bullet-}$ by the reaction of $O_2^{\bullet-}$ and PS. The results are consistent with these obtained in EPR studies.

The results presented in Figs. 1 and 2 indicated that $O_2^{\bullet-}$ radical generated by MNPs can activate PS to generate more $SO_4^{\bullet-}$ radical. Although the reactivity of $O_2^{\bullet-}$ was lower than that of other radical species such as •OH and $SO_4^{\bullet-}$ in aqueous solution, it was greatly enhanced in the presence of solid surface, especially when the solid particles size were smaller than 20 nm, which could cause quantum confinement effects [17]. Quantum confinement can result in altering the surface free energy and the $O_2^{\bullet-}$ solvation shell, which may enhance the reactivity of reactants [17,24]. Therefore, the reactivity of $O_2^{\bullet-}$ with PS was greatly enhanced in the presence of MNPs, which resulted in the formation of more $SO_4^{\bullet-}$. Similar phenomenon has been observed elsewhere [40]. For example, Jones et al. [40] investigated the reaction of $O_2^{\bullet-}$ with silver ions (Ag^+), and found that the reactivity of $O_2^{\bullet-}$ was greatly enhanced in the presence silver nanoparticles. The mechanism of the generation of ROS in Fe(II) or ZVI was elucidated in previous research studies according to Eqs. (1)–(5) [30]. Therefore, it is hypothesized that the suggested mechanism of the generation of $O_2^{\bullet-}$ in MNPs is similar to these of Fe(II) or ZVI, and is that the sorbed or lattice Fe(II) of MNPs provides an electrons to O_2 to give $O_2^{\bullet-}$. According to Eqs. (1)–(5), pH, Fe(II) and O_2 could influence the generation of $O_2^{\bullet-}$, which ultimately affects the production of $SO_4^{\bullet-}$ by PS activated with MNPs. Therefore, the effects of pH, Fe(II) and O_2 should be considered.

3.2. Effect of adsorbed Fe(II) on the degradation of PCB28 by PS/MNPs and the generation of radical species by MNPs

Previous studies have been reported that the adsorbed Fe(II) on MNPs could increase its reductive reactivity and this behavior was attributed to the fact that the adsorbed Fe(II) could increase the electron density of MNPs surface and lower the redox potential of surface-bound Fe(II), which in turn may promote the electron transfer to target contaminant molecules to initiate the dechlorination reaction [14,15,41]. But none of these studies have investigated the generation of ROS in these processes, and the role of ROS was not fully elucidated. Therefore, it is necessary to investigate the effect of adsorbed Fe(II) on the degradation of PCB28 in PS/MNPs system, as well as the generation of $O_2^{\bullet-}$ by MNPs.

Fig. 3(a) shows that 95% of PCB28 was degraded within 120 min by PS/MNPs-Fe(II), while only 75% of PCB28 was degraded without Fe(II). Even prolonging the reaction time up to 240 min, only 90% of the PCB28 was degraded by PS/MNPs in the absence of Fe(II). The results indicate that the presence of Fe(II) could greatly enhance the degradation of PCB28 by PS/MNPs. This is due to the generation of more $O_2^{\bullet-}$ to activate PS to produce additional amount of $SO_4^{\bullet-}$ in the presence of Fe(II), which enhances the transformation rates of PCB28. In addition, the degradation efficiency of PCB28 was approximately 50% in MNPs-Fe(II) in the absence of PS, which may be ascribed to the radical species such as •OH and hydroperoxyl radical ($HO_2^{\bullet-}$) or reductive dechlorination by Fe(II).

To identify the roles of radical species and reductive dechlorination in these processes, experiments were performed in the presence of 10 mM ethanol, which acts a scavenger of $SO_4^{\bullet-}$ and •OH in MNPs-Fe(II), under otherwise identical reaction conditions. The results presented in Fig. 3(a) show that only 17% of PCB28 was degraded by MNPs-Fe(II) in the presence of ethanol, which was slightly higher than that degraded by MNPs without Fe(II) (12%, Fig. 1(a)). This suggests that degradation of PCB28 was mainly ascribed to the oxidation by ROS, instead of the reductive dechlorination degradation by Fe(II). In addition, the ratio of $[O_2^{\bullet-}]/[HO_2^{\bullet-}]$ was approximately 100/1 at pH 6.8 and 1000/1 at pH 7.8 [42]. Therefore, the contribution of $HO_2^{\bullet-}$ to the degradation of PCB28 was limited under the present reaction conditions, and •OH was mainly ROS responsible for the degradation of PCB28.

To further confirm this conclusion, EPR was used to identify radical species generated by MNPs-Fe(II). As illustrated in Fig. 3(b), the formation of DMPO-O_2 signal in MNPs-Fe(II) was significantly higher than that in MNPs, indicating the formation of more $O_2^{\bullet-}$ by MNPs-Fe(II). Furthermore, new radical signals were observed

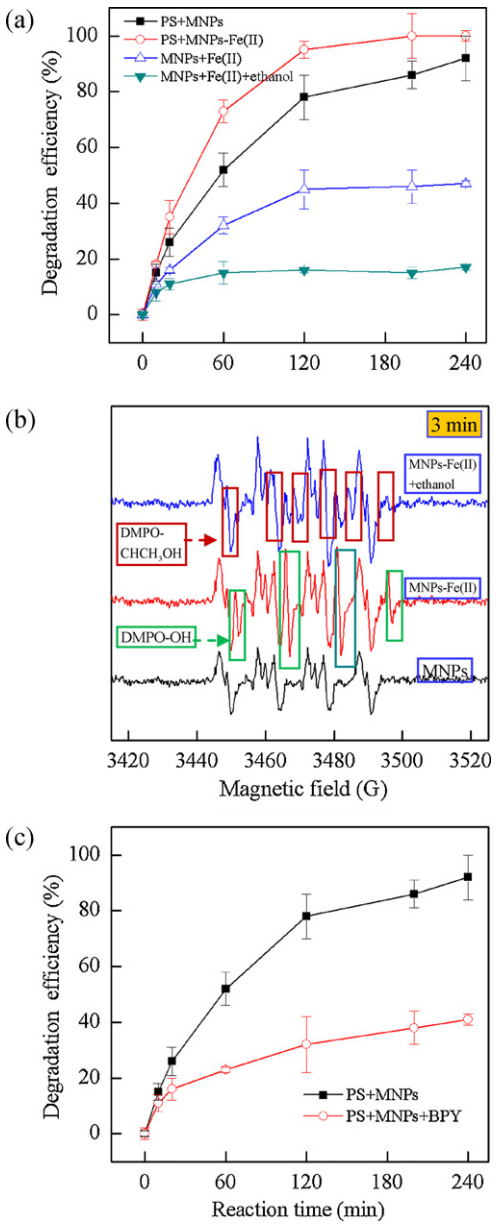

Fig. 3. Effect of the sorbed Fe(II) on MNPs surface on the degradation of PCB28 by PS/MNPs-Fe(II) (a). EPR spectrum of MNPs-Fe(II) in the presence of 10 mM ethanol (b). Degradation of PCB28 by PS/MNPs in the presence of 1.0 mM BPY (c). Reaction conditions: [PS] = 2.0 mM, [PCB28] = 2.5 μM, [MNPs] = 1.0 g/L, [ethanol] = 10 mM, [DMPO] = 0.10 M, 25 °C, pH 7.0 and reaction for 4 h.

(a_N = 14.4 G, a_H = 15.2 G), which was characteristics of DMPO-OH adducts, verifying the generation of •OH in this process [43]. However, many investigators found that the reaction of Fe(II) or Fe(III) with DMPO or the decomposition of DMPO-OOH adducts could also produce DMPO-OH signal [42], therefore, ethanol was used as scavenger to identify •OH radical. As shown in Fig. 3(b), the formation of DMPO-OH markedly decreased in the presence of 10 mM ethanol due to the scavenging reaction, meanwhile, a new signal appeared, which was characteristics of $^{\bullet}CHCH_3OH$ radical DMPO adducts (a_H = 22.7 G, a_N = 15.7 G). The results indicated that the formation of DMPO-OH signal was resulted from the reaction of •OH with DMPO instead of the reaction of Fe(II) or Fe(II) with DMPO or the decomposition of DMPO-OOH.

The mechanism of the generation of •OH can be explained as follows. According to Eqs. (2) and (4), the reaction of $O_2^{\bullet-}$ and hydrogen ions (H^+) and Fe(II) could produce H_2O_2, although its concentration was relatively low at around neutral pH. Therefore, in the presence of enough Fe(II), •OH could be produced as described in Eq. (5) through Fenton reactions. In contrast, in the MNPs solution without Fe(II), •OH could not be produced since the concentration of Fe(II) was too low to activate the H_2O_2. These results indicate that the role of the ROS should be considered when evaluating the reductive dechlorination of contaminants by Fe(II) sorbed on the metal oxides surface.

Experiments were also conducted in the presence of 1.0 mM of 2,2′-bipyridine (BPY), which would complex with Fe(II) and thus hinder the transfer of electrons to O_2. Fig. 3(c) shows that the degradation efficiency of PCB28 decreased from 90% to 40% in the presence of BPY, indicating that the BPY greatly inhibited the degradation of PCB28 by MNPs/PS. This is a clear indication that the reaction of lattice or bound Fe(II) with oxygen is essential for the generation of $O_2^{\bullet-}$. Moreover, the formation of DMPO-O_2 was also inhibited in the presence of BPY (Fig. S5), and the results are consistent with the above discussion. Similar results were also observed by Katsoyiannis et al. [31] who used ZVI combined with Fe(II) for the oxidation of As(III), and found that the presence of BPY significantly inhibited the oxidation of As(III).

3.3. The roles of pH in the degradation of PCB28 by PS/MNPs and the generation of radical species by MNPs

Previous studies reported that the pH strongly influenced magnetite reactivity as well as the rate of $O_2^{\bullet-}$ disproportionation, which might affect the activation of PS by MNPs [16,40,44]. Thus, the effects of pH on the degradation of PCB28 as well as the generation of radical species were studied. Fig. 4(a) shows the observed pseudo-first-order rate constant (k_{obs}) of PCB28 as a function of pH. When the pH was below 5.0, the k_{obs} increased with increasing pH. However, the k_{obs} decreased with further increasing pH from 5.0 to 7.0, and then increased from 7.0 to 11.0, finally, decreased as pH increased to 12.0.

$O_2^{\bullet-}$ drives the activation of PS by MNPs, thus, the generation of radical species as a function of pH was investigated in the MNPs solution (Fig. 4(b)). Interestingly, the formation of •OH radicals was observed in MNPs solution at pH 5.0. According to Eqs. (2) and (4), lowering the pH favored the formation of H_2O_2 and the Fe(II) dissolved from MNPs, which resulted in the formation of •OH. Both •OH and $SO_4^{\bullet-}$ would account for the degradation of PCB28, therefore, the k_{obs} of PCB28 at pH 5.0 was higher than that of other pH values. Fig. 4(c) shows that the formation of the DMPO-OH decreased as pH increased from 3.0 to 5.0, and at pH above 7.0, the signal of DMPO-OH completely disappeared. This is attributed to the fact that dissolved Fe(II) from the MNPs is too low to generate •OH at relatively high pH. Theoretically, lowering pH favors the transformation of PCB28 due to the generation of more radical species, but k_{obs} values of PCB28 at pH 3.0 and 4.0 were lower than that at pH 5.0. This phenomenon is due to excess of radical species; radical self-scavenging can take place according to the following reactions.

$$SO_4^{\bullet-} + SO_4^{\bullet-} \rightarrow S_2O_8^{2-} \quad (7)$$

$$^{\bullet}OH + {}^{\bullet}OH \rightarrow H_2O_2 \quad (8)$$

$$Fe^{2+} + {}^{\bullet}OH \rightarrow FeOH^{2+} \quad (9)$$

Fig. 4(c) also shows that the formation of DMPO-O_2 increased as pH increased, which resulted in the activation of PS to produce more $SO_4^{\bullet-}$. Therefore, the k_{obs} of PCB28 increased with increasing pH from 7.0 to 11.0. Similar results were observed elsewhere [45].

Two reasons can explain that the increasing pH favored the generation of $O_2^{\bullet-}$, which resulted in an increase of the degradation efficiency of PCB28 with an increase of pH 7.0 to 11.0. First,

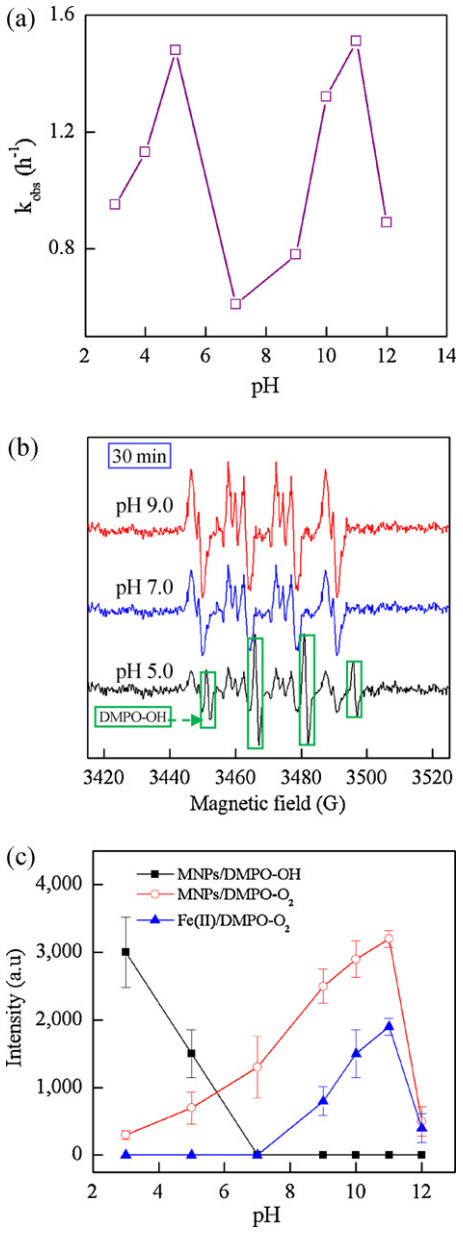

Fig. 4. The k_{obs} of PCB28 as function of pH values (a). The EPR spectrum of MNPs at different pH (5.0, 7.0 and 9.0) at 30 min (b). Intensity of the formation of DMPO adducts in MNPs as function of pH values (c). The EPR data were obtained from the MNPs solution at different pH values at 30 min. Reaction conditions: [PS] = 2.0 mM, [PCB28] = 2.5 μM, [MNPs] = 1.0 g/L, 25 °C, pH 7.0, [DMPO] = 0.1 M and reaction for 4 h.

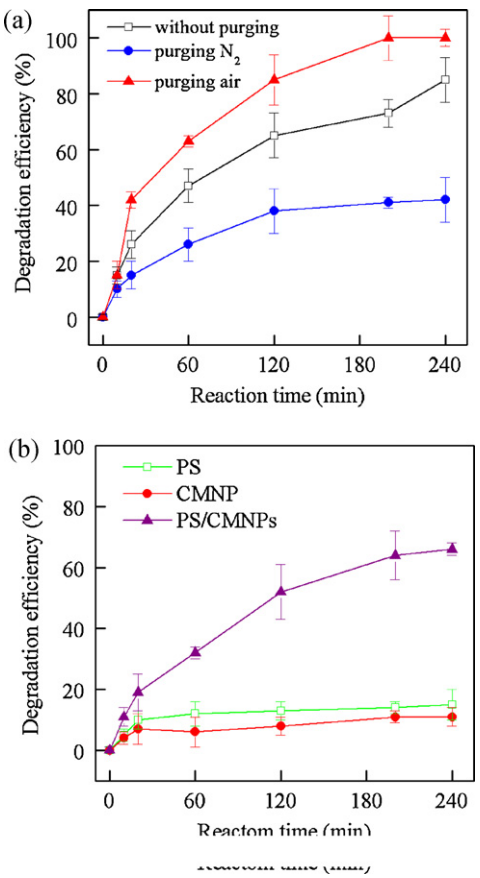

Fig. 5. Effects of dissolved oxygen on the degradation of PCB28 by PS/MNPs (a). The solution was treated by purging with N_2, air for 1 h and without purging before initial the reaction. The activation of PS by commercial magnetite nanoparticles for the degradation of PCB28 (b). Reaction conditions: [PS] = 2.0 mM, [PCB28] = 2.5 μM, [MNPs] = 1.0 g/L, 25 °C, pH 7.0, and reaction for 4 h.

the evolution of $O_2^{\bullet-}$ to H_2O_2 was pH-dependent according to Eqs. (2) and (4). Thus, increasing pH suppressed reaction Eqs. (2) and (4), and resulted in the formation of more $O_2^{\bullet-}$, which favored the activation of PS for the degradation of PCB28. Second, the different species of Fe(II) have different reaction rate constants with O_2. For example, the reaction rate constants of Fe(II), $FeOH^+$ and $Fe(OH)_2^0$ with O_2 were 4.95×10^{-1}, 4.17×10^2 and $5.25 \times 10^7\ M^{-1}\ s^{-1}$ [30], respectively. Moreover, the distribution of Fe(II) species is pH-dependent. Therefore, the generation of $O_2^{\bullet-}$ was also pH-dependent. Fig. S6 shows the distribution of Fe(II) (0.1 mM) species as a function of pH values, and the equilibrium calculations were performed using the software MINEQL+ with the stability constants provided in the database. The results indicate that the fractions of $FeOH^+$ and $Fe(OH)_2^0$ increased with increasing pH, which have larger reaction rate constants with O_2, compared to Fe^{2+}, resulting in the formation of more $O_2^{\bullet-}$. Consequently, it was found that the k_{obs} of PCB28 increased as pH increased from 7.0 to 11.0.

Experiments were also performed to investigate the generation of ROS in the Fe(II) (2.0 mM) solution as a function of pH. As shown in Fig. 4(c), we could not detect any DMPO adducts signals at pH values below 7.0 because homogeneous Fe(II) oxidation by O_2 is also strongly pH dependent. This is consistent with previous studies that indicated the oxidation of Fe(II) could be neglected in a homogeneous solution at pH below 6.5 [33]. For example, the half-life of reaction of Fe(II) with O_2 is approximately 45 h at pH 6.0, 4.5 h at pH 6.5, and 27 min at pH 7.0 under homogeneous conditions [46]. However, formation of DMPO-O_2 signal was observed at pH 9.0, although its intensity was extremely low. As pH ranging from 9.0 to 11.0, the intensity increased rapidly; while production of solid precipitate, including $Fe(OH)_2$ and $Fe(OH)_3$. The solid precipitate facilitates the generation of superoxide radical and enhances the reactivity of superoxide radical based on surface catalysis. At pH 12.0, the formation of DMPO-O_2 decreased rapidly. These results were consistent with the above discussion on the formation of radical species in MNPs-Fe(II).

3.4. Effects of dissolved oxygen and commercial magnetite nanoparticles (CMNPs) on the degradation of PCB28

Fig. 5(a) shows the degradation efficiency of PCB28 was 100% within 200 min under air purging, while only 71% and 40% of PCB28 was degraded without purging and N_2 purging, respectively, under identical reaction conditions, indicating that increasing O_2

concentration in the reaction solution greatly increased the degradation efficiency of PCB28. This is due to fact that the increase of O_2 concentration led to generation of more $O_2^{\bullet-}$ to activate the PS to produce $SO_4^{\bullet-}$, which favored the transformation of PCB28. To testify this hypothesis, the effects of O_2 concentration on the formation of DMPO-O_2 signal were investigated by EPR. Fig. S7 shows that the formation of DMPO-O_2 signal by MNPs with air purging was significantly higher than that in the case of N_2 purging and without purging. Similar phenomenon was observed by Kim et al. [21], who found that the generation of ROS by ZVI under air-saturated conditions was greater than that generated under deaerated conditions.

Additionally, we also used commercial magnetite nanoparticles (CMNPs) for the activation of PS for the degradation of PCB28 to compare with the MNPs used in this study. Experiments were performed with identical reaction conditions. Fig. 5(b) shows that 60% of PCB28 was degraded in PS/CMNPs, while approximately 10% of PCB28 was degraded in PS or CMPNs alone. The k_{obs} of PCB28 degraded by MNPs/PS and CMNPs/PS were 0.61 and 0.27 h^{-1}, respectively. Normalizing the k_{obs} based on surface area, the data were 0.0074 g m^{-2} h^{-1} for MNPs/PS, and 0.0044 g m^{-2} h^{-1} for CMNPs/PS. The results indicate that the CMNPs could also activate PS for the degradation of PCB28, although its catalytic efficiency was lower than that of MNPs prepared in this study. Two explanations could rationalize this behavior. The first concerns the size of CMNPs, which was larger than that of MNPs, thus, its reactivity was lower than MNPs. Many studies also reported that the smaller the size of magnetite particles is, the higher is their reactivity [17]. Second, the surface of CMNPs was modified with some polymers, such as oleic acid, to prevent particle aggregation, which led to decreasing in their reactivity. Similar to the MNPs, we also observed the generation of $O_2^{\bullet-}$ in CMNPs suspension (Fig. S8).

4. Conclusions

This study suggests that the activation of persulfate (PS) by MNPs could degrade PCB28 efficiently in aqueous solution. The mechanism involves generation of $O_2^{\bullet-}$ radical in MNPs, which reacts with persulfate anion to produce $SO_4^{\bullet-}$ radical, a significant species involved in the degradation of PCB28 in this process. EPR technique and quenching studies were used to identify the radical species of these processes. Increasing the pH and dissolved oxygen concentration led to increasing in the amount of $O_2^{\bullet-}$ radicals generated by MNPs. Sorption of Fe(II) on MNPs surface favored the generation of $O_2^{\bullet-}$ and $^{\bullet}OH$. The CMNPs also exhibited excellent catalytic reactivity toward PS activation and subsequent degradation of PCB28. The findings of this study provide new insights into the mechanism of heterogeneous catalysis based on MNPs and the reactivity of MNPs toward environmental contaminants. The findings of this study also provide a new insight into the understanding of the reactivity of Fe(II) sorbed on metal oxides for the degradation of contaminants.

Acknowledgments

The authors gratefully acknowledge the support of the National Basic Research and Development Program Foundation number (2013CB934300) and National Natural Science Foundation of China (41125007).

Appendix A. Supplementary data

Supplementary data associated with this article can be found, in the online version, at http://dx.doi.org/10.1016/j.apcatb.2012.09.042.

References

[1] G.P. Anipsitakis, D.D. Dionysiou, Environmental Science and Technology 37 (2003) 4790–4797.
[2] M.G. Antoniou, A.A. De la Cruz, D.D. Dionysiou, Applied Catalysis B: Environmental 96 (2009) 290–298.
[3] G.P. Anipsitakis, D.D. Dionysiou, M.A. Gonzalez, Environmental Science and Technology 40 (2006) 1000–1007.
[4] G.P. Anipsitakis, D.D. Dionysiou, Applied Catalysis B: Environmental 54 (2004) 155–163.
[5] A.L. Teel, M. Ahmad, R.J. Watts, Journal of Hazardous Materials 196 (2011) 153–159.
[6] J.C. Yan, M. Lei, L.H. Zhu, M.N. Anjum, J. Zou, H.Q. Tang, Journal of Hazardous Materials 186 (2011) 1398–1404.
[7] A. Rastogi, S.R. Al-Abed, D.D. Dionysiou, Applied Catalysis B: Environmental 85 (2009) 171–179.
[8] A. Rastogi, S.R. Al-Abed, D.D. Dionysiou, Water Research 43 (2009) 684–694.
[9] K.C. Huang, Z.Q. Zhao, G.E. Hoag, A. Dahmani, P.A. Block, Chemosphere 61 (2005) 551–560.
[10] G.D. Fang, D.D. Dionysiou, Y. Wang, S.R. Al-Abed, D.M. Zhou, Journal of Hazardous Materials 227-228 (2012) 394–401.
[11] G.D. Fang, D.D. Dionysiou, D.M. Zhou, Y. Wang, X.D. Zhu, J.X. Fan, L. Cang, Y.J. Wang, Chemosphere (2012), http://dx.doi.org/10.1016/j.chemosphere.2012.07.047.
[12] M. Elsner, R.P. Schwarzenbach, S.B. Haderlein, Environmental Science and Technology 38 (2004) 799–807.
[13] T.B. Hofstetter, R.P. Schwarzenbach, S.B. Haderlein, Environmental Science and Technology 37 (2003) 519–528.
[14] K.B. Gregory, P. Larese-Casanova, G.F. Parkin, M.M. Scherer, Environmental Science and Technology 38 (2004) 1408–1414.
[15] C.A. Gorski, M.M. Scherer, Environmental Science and Technology 43 (2009) 3675–3680.
[16] K.M. Danielsen, K.F. Hayes, Environmental Science and Technology 38 (2004) 4745–4752.
[17] P.J. Vikesland, A.M. Heathcock, R.L. Rebodos, K.E. Makus, Environmental Science and Technology 41 (2007) 5277–5283.
[18] R.L. Rebodos, P.J. Vikesland, Langmuir 26 (2010) 16745–16753.
[19] T.B. Scott, G.C. Allen, P.J. Heard, M.G. Randell, Geochimica et Cosmochimica Acta 69 (2005) 5639–5646.
[20] D.M. Singer, S.M. Chatman, E.S. Ilton, K.M. Rosso, J.F. Banfield, G.A. Waychunas, Environmental Science and Technology 46 (2012) 3821–3830.
[21] J.Y. Kim, C. Lee, D.C. Love, D.L. Sedlak, J. Yoon, K.L. Nelson, Environmental Science and Technology 45 (2011) 6978–6984.
[22] C. Lee, J.Y. Kim, W.I. Lee, K.L. Nelson, J. Yoon, D.L. Sedlak, Environmental Science and Technology 42 (2008) 4927–4933.
[23] O. Furman, Reactivity of oxygen species in homogeneous and heterogeneous aqueous environments, Ph.D. Dissertation, Washington State University, Washington, 2009.
[24] O. Furman, D.F. Laine, A. Blumenfeld, A.L. Teel, K. Shimizu, I.F. Cheng, R.J. Watts, Environmental Science and Technology 43 (2009) 1528–1533.
[25] S.H. Joo, A.J. Feitz, T.D. Waite, Environmental Science and Technology 38 (2004) 2242–2247.
[26] S.H. Joo, A.J. Feitz, D.L. Sedlak, T.D. Waite, Environmental Science and Technology 39 (2005) 1263–1268.
[27] C.R. Keenan, D.L. Sedlak, Environmental Science and Technology 42 (2008) 1262–1267.
[28] S.H. Kang, W. Choi, Environmental Science and Technology 43 (2008) 878–883.
[29] J. Lee, J. Kim, W. Chio, Environmental Science and Technology 41 (2007) 3335–3340.
[30] C.R. Keenan, Reactive oxidant generation by nanoparticulate zero-valent iron: contaminant oxidation and toxicity, Ph.D. Dissertation, University of California, Berkeley, 2010.
[31] I.A. Katsoyiannis, T. Ruettimann, S.J. Hug, Environmental Science and Technology 42 (2008) 7424–7430.
[32] S.J. Hug, L. Canonica, M. Wegelin, D. Gechter, U.V. Gunten, Environmental Science and Technology 35 (2001) 2114–2121.
[33] K. Pecher, S.B. Haderlein, R.P. Schwarzenbach, Environmental Science and Technology 36 (2002) 1734–1741.
[34] S.X. Zhang, X.L. Zhao, H.Y. Niu, Y.L. Shi, Y.Q. Cai, G.B. Jiang, Journal of Hazardous Materials 167 (2009) 560–566.
[35] L.J. Xu, J.L. Wang, Applied Catalysis B 123–124 (2012) 117–126.
[36] F.Y. Cheng, C.H. Su, Y.S. Yang, C.S. Yeh, C.Y. Tsai, C.L. Wu, M.T. Wu, D.B. Shieh, Biomaterials 26 (2005) 729–738.
[37] A. Buchholz, C. Laskov, S.B. Haderlein, Environmental Science and Technology 45 (2011) 3355–3360.
[38] O.S. Furman, A.L. Teel, R.J. Watts, Environmental Science and Technology 44 (2010) 6423–6428.
[39] Z. Nie, Q. Tian, Y.P. Liu, Y. Liu, Magnetic Resonance in Chemistry 44 (2006) 38–44.
[40] A.M. Jones, S. Garg, D. He, A.N. Pham, T.D. Waite, Environmental Science and Technology 45 (2011) 1428–1434.
[41] J.E. Amonette, D.J. Workman, D.W. Kennedy, J.S. Fruchter, Y.A. Gorby, Environmental Science and Technology 34 (2000) 4606–4613.

[42] M.D. Paciolla, The Evolution of Reactive Oxygen Species Induced by Humic Acid and Their Implications on Biological Activity and Oxidative Stress, Temple University, Philadelphia, 2001.
[43] M.M. Ye, Z.L. Chen, X.W. Liu, Y. Ben, J.M. Shen, Journal of Hazardous Materials 167 (2009) 1021–1027.
[44] J. Klausen, S.P. Troeber, S.B. Haderlein, R.P. Schwarzenbach, Environmental Science and Technology 29 (1995) 2396–2404.
[45] S. L. Smith-Tembe, Abiotic reduction of nitrite, uranium(VI), and chlorinated ethenes by iron(II) species, Ph.D. Dissertation, The University of Iowa, Iowa, 2006.
[46] D.W. King, H.A. Lounsbury, F.J. Millero, Environmental Science and Technology 29 (1995) 818–824.